Proof-of-Concept for a Real-Time ECG-Guided Framework for Ventricular Tachycardia Exit Site Localization and Catheter Navigation

Noah Emmert[1], Konstantinos N Aronis[2], and Shijie Zhou[3]

[1]Computer Science and Software Engineering, Miami University, Oxford, United States
[2]School of Medicine, Johns Hopkins Hospital, Baltimore, United States
[3]Biomedical Engineering, Worcester Polytechnic Institute, Worcester, United States

Abstract

Accurate localization of ventricular tachycardia (VT) exit sites is essential for effective ablation therapy. However, existing pace mapping (PM) techniques lack real-time, quantitative feedback, making procedures highly operator-dependent. We propose a novel, data-driven framework for real-time VT exit site localization and catheter navigation using standard 12-lead ECG signals. By formulating the task as a linear inverse problem, we employ a machine learning pipeline that estimates spatial displacements based on QRS integral features. Four regression models—multivariate, Ridge, Lasso, and Elastic Net—were evaluated on data from four patients undergoing VT ablation. Sparse regression models, particularly Elastic Net without intercept, achieved the best performance, yielding a mean localization error of ***11.5 ± 3.1 mm*** *using only 14 pacing sites. The system provides continuous directional guidance, iteratively refining predictions and guiding catheter movement toward the VT origin. This study demonstrates the feasibility of an ECG-based, real-time navigation tool and supports its potential integration into clinical electrophysiology workflows to enhance procedural precision and reduce reliance on operator experience.*

1. Introduction

Ventricular tachycardia (VT) is a potentially fatal arrhythmia if not treated promptly [1]. Catheter ablation has proven effective in certain patients [2], but identifying VT exit sites remains a major clinical challenge. Pace mapping (PM) is one of the major clinical mapping techniques used for VT localization, in which the operator compares the morphology of paced QRS complexes with the clinical VT morphology on standard ECGs [3]. While effective in skilled hands, this approach is inherently subjective and heavily dependent on operator experience.

VT localization is still operator-driven, time-consuming, and qualitative [4]. Learning to link ECG morphologies to anatomy takes years, and the lack of quantitative, real-time feedback prolongs procedures and lowers success rates, particularly for newer operators [5], [6].

To address these limitations, we present a novel, **proof-of-concept framework** that leverages routine 12-lead ECG data to localize VT exit sites and guide catheter navigation **in real time**. After each pacing stimulus, the proposed framework predicts the three-dimensional displacement to the exit site; the catheter is steered along this vector, and the newly reached position becomes the next pacing location. The loop repeats until convergence, mirroring the clinical PM workflow while adding objective, data-driven guidance.

We employed multiple regression models with various regularization techniques to estimate spatial displacements from ECG-derived features—marking an important step toward integrating machine learning into clinical electrophysiology through real-time guidance that enhances efficiency, reduces operator dependency, and improves the reproducibility of VT ablation.

2. Methods

2.1. Study Population, Data Acquisition, and Preprocessing

Four patients undergoing catheter ablation for scar-related VT ($\approx$ 21 pacing sites each) were enrolled with informed consent and IRB approval. During procedures, intracardiac catheters marked pacing sites, and simultaneous 12-lead ECGs were recorded (0.05–100 Hz, 1000 Hz, 16-bit) for 7 s per site. A cloned ECG stream was routed to a secure workstation. Three-dimensional electro-anatomic maps were built; pacing sites with Stim-QRS $\leq$ 40 ms were retained. For each, the QRS complex (120 ms) was integrated across eight independent leads (I, II, V1–V6) as in [7], [8].

2.2 QRS Time-Integral and Spatial Displacement Vectors

For pacing sites P_i and P_j, the QRS Time-Integral Displacement Vector (QRSIDV) Q_{ij} was defined as:

$$Q_{ij} = q_j - q_i$$

where q_i and q_j are 8-lead QRS integral vectors for P_i and P_j respectively. This captures the change in electrical activation between two pacing sites. Corresponding spatial displacement vector D_{ij} was computed as:

$$D_{ij} = P_j - P_i$$

where P_i and P_j are the 3D anatomical coordinates of the pacing sites. QRSIDVs serve as predictors; spatial vectors are regression targets.

2.3 Linear Inverse Problem Formulation

The relationship between QRSIDVs and 3D spatial displacement vectors was modeled as a linear inverse problem, aiming to estimate spatial displacement vectors from observed ECG changes, as:

$$D_{ij} = A \cdot Q_{ij} + \epsilon$$

where A is the transformation matrix to be estimated, and ϵ accounts for noise and measurement variability. Due to the high dimensionality and potential multicollinearity among ECG features, this constitutes an ill-posed problem that may lack a unique or stable solution. To address this, we implemented and compared multiple regularized regression techniques—including multivariate linear regression, Lasso [9], Ridge [10], and Elastic Net [11]—to stabilize the estimation process and enhance model generalizability [9].

2.4 Transformation Matrix Calculation

To estimate the transformation matrix A, we applied and compared several regression techniques, with and without intercept terms (denoted as NI for "no intercept"), to evaluate the effect of bias:

1. Multivariate Linear Regression (Ordinary Least Squares, OLS): Minimizes the L2-norm of residuals. Simple but prone to overfitting with high-dimensional predictors.
2. Lasso Regression (L1 Regularization) [9]: Adds an L1 penalty to promote sparsity in A, effectively performing feature selection by identifying the most relevant ECG leads for predicting displacement.
3. Ridge Regression (L2 Regularization) [10]: Applies an L2 penalty to reduce multicollinearity and overfitting. Retains all features but shrinks coefficients.
4. Elastic Net Regression (combined L1 + L2) [11]: Balances the benefits of sparsity and coefficient shrinkage. The hybrid method is particularly effective when predictors are correlated [11].

All models were implemented in Python using Scikit-learn library. Regularization hyperparameters (λ) were tuned through five-fold cross-validation [12].

2.5 VT Exit Site Localization Pipeline

Once the transformation matrix A was learned, it was used to estimate the VT exit site. Specifically, the QRSIDV between a reference pacing site P_1 and the target VT beat was computed as $q_{VT} - q_{P_1}$. The predicted displacement vector D_{VT-P_1} was then calculated as:

$$D_{VT-P_1} = A \cdot (q_{VT} - q_{P_1})$$

The predicted VT exit site was then obtained by adding this displacement vector to the reference site:

$$P_{VT,est} = P_1 + D_{VT-P_1}$$

Predictions were mapped onto the nearest surface node via **Trimesh** library [13] to ensure anatomical consistency and enable visualization within the clinical mapping environment.

2.6 Directional Feedback for Navigation

To enable real-time catheter guidance, the predicted displacement vector was iteratively updated using QRSIDV's from newly added pacing sites. Unit vector D_{VT-P_1} provided directional guidance for catheter movement, while its magnitude $|D_{VT-P_1}|$ served as an estimate of distance to VT exit site. This allowed for progressive refinement of localization and navigation throughout the ablation procedure.

2.7 Simulated Prospective Analysis & Metrics

To evaluate clinical feasibility, we conducted a simulated prospective analysis on a representative patient set. The goal was to assess how different regression techniques would affect localization performance.

The simulation began with initial training set of four randomly selected pacing sites (max inter-site distance ≤ 30 mm) mimicking typical clinical practice where operators begin pacing in a localized region based on initial clinical assessment. **K-nearest neighbors (KNN)** strategy (k=1, Euclidean distance) was used to iteratively expand the training set and update transformation matrix A, progressively exploring broader VT-relevant regions. The following procedure was repeated until 14 available pacing sites were incorporated:

1. Predict VT exit site using the current training set.
2. Identify the nearest available pacing site to the predicted location.
3. Add the selected site to the training set.
4. Recalculate the transformation matrix A.

At each iteration, model predictions were stored for later evaluation of localization performance.

Localization accuracy was measured as Euclidean distance between predicted and actual VT exit sites. For

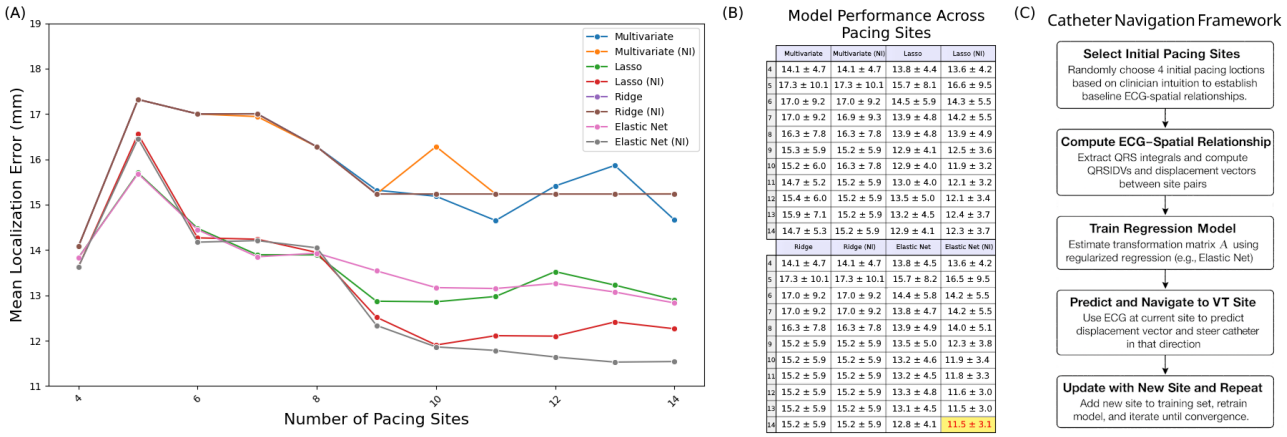

	Multivariate	Multivariate (NI)	Lasso	Lasso (NI)
4	14.1 ± 4.7	14.1 ± 4.7	13.8 ± 4.4	13.6 ± 4.2
5	17.3 ± 10.1	17.3 ± 10.1	15.7 ± 8.1	16.6 ± 9.5
6	17.0 ± 9.2	17.0 ± 9.2	14.5 ± 5.9	14.3 ± 5.5
7	17.0 ± 9.2	16.9 ± 9.3	13.9 ± 4.8	14.2 ± 5.5
8	16.3 ± 7.8	16.3 ± 7.8	13.9 ± 4.8	13.9 ± 4.9
9	15.3 ± 5.9	15.2 ± 5.9	12.9 ± 4.1	12.5 ± 3.6
10	15.2 ± 6.0	16.3 ± 7.8	12.9 ± 4.0	11.9 ± 3.2
11	14.7 ± 5.2	15.2 ± 5.9	13.0 ± 4.0	12.1 ± 3.2
12	15.4 ± 6.0	15.2 ± 5.9	13.5 ± 5.0	12.1 ± 3.4
13	15.9 ± 7.1	15.2 ± 5.9	13.2 ± 4.5	12.4 ± 3.7
14	14.7 ± 5.3	15.2 ± 5.9	12.9 ± 4.1	12.3 ± 3.7

	Ridge	Ridge (NI)	Elastic Net	Elastic Net (NI)
4	14.1 ± 4.7	14.1 ± 4.7	13.8 ± 4.5	13.6 ± 4.2
5	17.3 ± 10.1	17.3 ± 10.1	15.7 ± 8.2	16.5 ± 9.5
6	17.0 ± 9.2	17.0 ± 9.2	14.4 ± 5.8	14.2 ± 5.5
7	17.0 ± 9.2	17.0 ± 9.2	13.8 ± 4.7	14.2 ± 5.5
8	16.3 ± 7.8	16.3 ± 7.8	13.9 ± 4.9	14.0 ± 5.1
9	15.2 ± 5.9	15.2 ± 5.9	13.5 ± 5.0	12.3 ± 3.8
10	15.2 ± 5.9	15.2 ± 5.9	13.2 ± 4.6	11.9 ± 3.4
11	15.2 ± 5.9	15.2 ± 5.9	13.2 ± 4.5	11.8 ± 3.3
12	15.2 ± 5.9	15.2 ± 5.9	13.3 ± 4.8	11.6 ± 3.0
13	15.2 ± 5.9	15.2 ± 5.9	13.1 ± 4.5	11.5 ± 3.0
14	15.2 ± 5.9	15.2 ± 5.9	12.8 ± 4.1	11.5 ± 3.1

Figure 1. (A) Mean localization error (mm) for each regression method as pacing sites increase (4 to 14) under standard and no-intercept (NI) conditions. (B) Mean localization error ± SD (mm), by method and pacing site count, with best method's final iteration highlighted. (C) Flowchart of the iterative computational and prospective clinical workflow.

each training set configuration, mean localization error and standard deviation were computed as the average and standard deviation of patient-level means, respectively, to account for inter-patient variability.

3. Results

3.1 Localization Accuracy with Different Regression Methods

Across all pacing-site configurations, sparse models (Lasso, Elastic Net) outperformed multivariate and Ridge regression (Fig. 1). With four pacing sites, errors were similar (13.6-14.1 mm). However, as additional pacing sites were incorporated, sparse models improved most: Elastic Net (NI) reached 11.5 ± 3.1 mm at 14 pacing sites, Lasso (NI) 12.3 ± 3.7 mm. Convergence around 11-12 pacing sites suggests the transformation matrix A achieved adequate rank for reliable spatial mapping. Ridge remained higher at 15.2 ± 5.9 mm, while multivariate regression had the largest final errors (14.7 ± 5.3 mm with intercept, 15.2 ± 5.9 mm NI). NI slightly benefited sparse models but mildly worsened multivariate regression, indicating overfitting in high-dimensional space. NI made no difference for Ridge. These differences are visualized in **Figure 1**, which compares the mean localization accuracy for all models with and without intercept.

3.2 Effect of Training Set Size on Localization Accuracy

Adding pacing sites reduced error, especially for sparse models. Starting with four pacing sites (max inter-site distance ≤ 30 mm), KNN-guided inclusion lowered Elastic Net (NI) error from 13.6 ± 4.2 mm (4 sites) to 11.5 ± 3.1 mm (14 sites); Lasso (NI) error dropped from 13.6 ± 4.2 mm to 12.3 ± 3.7 mm over the same range. Improvements

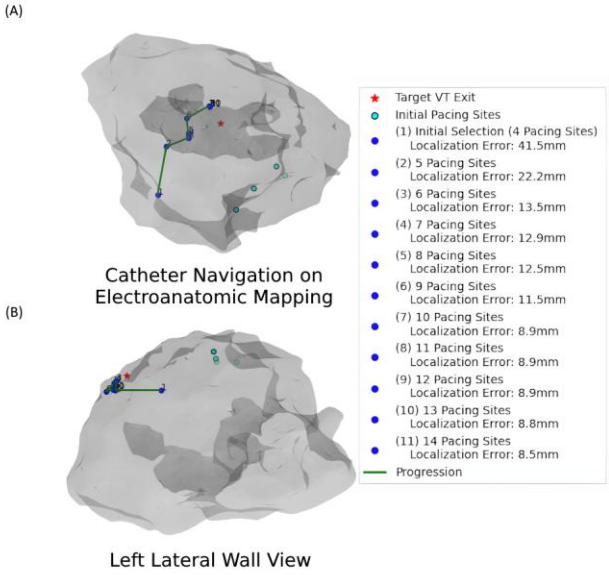

Figure 2. A representative case. (A) Left ventricle rendering of the iterative procedure where directional feedback guides catheter navigation to VT exit. (B) Left lateral wall view of directional feedback.

plateaued after 12-14 sites. Ridge changed little with added data, mirroring its overall stability but lower accuracy.

4. Discussion

This study presents a novel methodology for real-time localization of ventricular tachycardia (VT) exit sites from standard 12-lead ECGs. Framing the task as a linear inverse problem to solve with sparse regression yields quantitative, directional feedback for automated catheter navigation, reducing reliance on operator experience.

4.1 Comparative Analysis of Regression Techniques

Sparse models—Lasso and Elastic Net—consistently gave the lowest localization error by selecting informative leads and time windows while limiting overfitting. Ridge remained stable but lacked this selectivity, and unregularized multivariate regression overfit as training size grew. These findings align with prior literature on ECG imaging [14]. Though error drop from 4 to 14 pacing sites is modest, the method enables automated, directional guidance that may reduce unnecessary pacing. A small but consistent error increase from 4 to 5 sites occurs likely due to initial sites being selected at random. Results converged as more pacing sites were added after 12 to 14. This is likely due to limitations of available data but may also suggest that additional pacing sites beyond this threshold provide diminishing returns in accuracy improvement.

4.2 Clinical Relevance and Integration

The achieved localization accuracy—11.5 ± 3.1 mm using Elastic Net (NI)—demonstrates this method's feasibility for guiding catheter movement during pace mapping. KNN-based iterative updates mirror clinical practice: each prediction directs the next pacing site, enabling on-the-fly refinement until converging on a single location. Because the algorithm runs using a data-driven approach with standard ECGs and existing 3-D mapping systems—direction vectors are simply projected onto the cardiac mesh—requires no extra hardware and is accessible across centers and operator experience levels. Future work could explore advanced site selection strategies, such as Bayesian optimization or active learning, but real-time computational constraints must be balanced against potential accuracy gains.

5. Limitations and Conclusions

The study used a small dataset of four patients—adequate for proof-of-concept but insufficient for broad VT generalizability. Future studies should incorporate larger, more diverse cohorts to confirm robustness and clinical value. The in-silico design may bias performance: during iterative KNN updates some predicted pacing sites overlapped the training set, potentially inflating accuracy. The method assumes consistent 12-lead ECG electrode placement, which may vary in clinical settings and differ by patient sex due to anatomical variation. While our small cohort was insufficient to assess sex-specific effects, larger, more diverse datasets could enable adjustment strategies that further improve robustness. A prospective implementation—where predictions guide acquisition of new, previously unvisited pacing sites—would better reflect real-word clinical usage and offer a stricter test.

This work demonstrates the feasibility of using sparse regression models and ECG-derived features for real-time VT localization and catheter navigation with clinically meaningful accuracy, continuous feedback, and an update loop mirroring catheter-lab practice. If validated in larger prospective studies, the method could streamline VT ablation by improving speed, precision, and accessibility.

References

[1] W. G. Stevenson and K. Soejima, "Catheter ablation for ventricular tachycardia," *Circulation*, vol. 115, no. 21, pp. 2750–2760, May 2007.

[2] F. E. Marchlinski *et al.*, "Long-term success of irrigated radiofrequency catheter ablation of sustained ventricular tachycardia: Post-approval THERMOCOOL VT trial," *J. Am. Coll. Cardiol.*, vol. 67, no. 6, pp. 674–683, Feb. 2016.

[3] E. M. Aliot *et al.*, "EHRA/HRS expert consensus on catheter ablation of ventricular arrhythmias," *Heart Rhythm*, vol. 6, no. 6, pp. 886–933, Jun. 2009.

[4] E. Anter, "Limitations and pitfalls of substrate mapping for ventricular tachycardia," *JACC Clin. Electrophysiol.*, vol. 7, no. 4, pp. 542–560, Apr. 2021.

[5] S. Kumar *et al.*, "Multicenter experience with catheter ablation for ventricular tachycardia in lamin A/C cardiomyopathy," *Circ. Arrhythm. Electrophysiol.*, vol. 9, no. 8, Aug. 2016, Art. no. e004357.

[6] F. Del Carpio Munoz, T. L. Buescher, and S. J. Asirvatham, "Three-dimensional mapping of cardiac arrhythmias," *Circ. Arrhythm. Electrophysiol.*, vol. 3, no. 6, pp. e6–e11, Dec. 2010.

[7] J. L. Sapp *et al.*, "Real-time localization of ventricular tachycardia origin from the 12-lead electrocardiogram," *JACC Clin. Electrophysiol.*, vol. 3, no. 7, pp. 687–699, Jul. 2017.

[8] S. Zhou, A. AbdelWahab, J. L. Sapp, J. W. Warren, and B. M. Horáček, "Localization of ventricular activation origin from the 12-lead ECG: A comparison of linear regression with non-linear methods of machine learning," *Ann. Biomed. Eng.*, vol. 47, no. 2, pp. 403–412, Feb. 2019.

[9] R. Tibshirani, "Regression shrinkage and selection via the lasso," *J. R. Stat. Soc. B*, vol. 58, no. 1, pp. 267–288, 1996.

[10] A. E. Hoerl and R. W. Kennard, "Ridge regression: Biased estimation for nonorthogonal problems," *Technometrics*, vol. 12, no. 1, pp. 55–67, Feb. 1970.

[11] H. Zou and T. Hastie, "Regularization and variable selection via the elastic net," *J. R. Stat. Soc. B*, vol. 67, no. 2, pp. 301–320, Apr. 2005.

[12] F. Pedregosa *et al.*, "Scikit-learn: Machine learning in Python," *J. Mach. Learn. Res.*, vol. 12, pp. 2825–2830, Nov. 2011.

[13] M. Dawson-Haggerty, *Trimesh*. (software), GitHub repository, 2019. [Online]. Available: https://github.com/mikedh/trimesh

[14] L. Li *et al.*, "Solving the inverse problem of electrocardiography for cardiac digital twins: A survey," *IEEE Rev. Biomed. Eng.*, vol. 18, pp. 316–336, 2025.

Address for correspondence:

Noah Emmert.
510 E. High St, Oxford, OH 45056.
emmertnp@miamioh.edu